

Article

Fabrication of a Novel MgO-B₂O₃-SiO₂-Zn Coating by Thermal Spraying

Zhan Yu ¹, Bo Song ², Ping Ma ^{3,*}, Wenhui Fan ^{1,*}, Enzhong Gong ¹, Yilun Sun ³, Yunlong Ding ² and Dongying Ju ^{1,2}

¹ School of Automobile and Transportation, Shenzhen Polytechnic, Shenzhen 518055, China; yuzhan198423@szpt.edu.cn (Z.Y.); enzhong@szpt.edu.cn (E.G.); dyju@sit.ac.jp (D.J.)

² Department of Material Science and Engineering, Saitama Institute of Technology, Saitama 369-0293, Japan; bos@sit.ac.jp (B.S.); ylding@sit.ac.jp (Y.D.)

³ Division of Consumer Goods and Environment, CCIC Southern Testing Co., Ltd., Shenzhen 518055, China; syl@ccic-set.com

* Correspondence: mp@ccic-set.com (P.M.); wenhuifan66@163.com (W.F.); Tel.: +86-755-26628305 (P.M.)

Abstract: In automotive technology, the proper use of thermal insulation materials helps improve the performance and life of internal equipment and reduce maintenance cost. In this study, plasma spraying and flame spraying are used to prepare and coat a new MgO-B₂O₃-SiO₂-Zn powder on the SUS304 substrate. The resulting coating as thermal insulation layer formed a networked microstructure between the substrates to improve the thermal insulation performance of the material. By validation of thermal radiation experiments, the thermal insulation effects of various ceramic powders were compared, the high-temperature and low-temperature thermal insulation materials for about 300 and 100 °C were determined, and the thermal insulation performance of the constructed material coatings was verified by analysis.

Keywords: surface engineering technology; thermal spraying technology; thermal insulation coating



Citation: Yu, Z.; Song, B.; Ma, P.; Fan, W.; Gong, E.; Sun, Y.; Ding, Y.; Ju, D. Fabrication of a Novel MgO-B₂O₃-SiO₂-Zn Coating by Thermal Spraying. *Coatings* **2021**, *11*, 907. <https://doi.org/10.3390/coatings11080907>

Academic Editor: Devis Bellucci

Received: 2 July 2021

Accepted: 26 July 2021

Published: 29 July 2021

Publisher's Note: MDPI stays neutral with regard to jurisdictional claims in published maps and institutional affiliations.



Copyright: © 2021 by the authors. Licensee MDPI, Basel, Switzerland. This article is an open access article distributed under the terms and conditions of the Creative Commons Attribution (CC BY) license (<https://creativecommons.org/licenses/by/4.0/>).

1. Introduction

In the design and use of automobiles, due to the heating characteristics of some of the power equipment itself, the entire vehicle cannot be maintained in a continuous and stable temperature environment to complete the driving task [1]. On the one hand, from the perspective of external stress adjustment, driving equipment and devices can be controlled by a certain environmental control system to maintain good working conditions; on the other hand, from the perspective of their own temperature retention capabilities, advanced insulation materials or surface engineering technology can be applied to enhance the insulation capacity of the equipment in the car [2]. This research is involved in thermal insulation coating technologies proposed in response to the above situation. It can be applied to plasma spraying and flame spraying, which can form a thermal insulation coating on the surface of metal substrate.

The spray technology is one of the surface engineering technologies [3,4]. This type of coating has better properties than the substrate material, expands its use range, prolongs the service life of its components, and saves resources [5,6]. Surface technology gives the material surface the required functions and improves its practical value. Typical surface properties required include corrosion resistance, wear resistance, lubricity, insulation, heat insulation, and wettability. The use of aluminum and titanium to increase the strength and thinning of steel as a countermeasure against global warming is very effective in improving fuel efficiency [7,8]. The surface function is controlled by the elements and structure of the coating film and the reaction product (rust) formed on the surface. How to accurately evaluate and control these is the key to creating a function. Even tiny defects, impurities, and disorder of atomic arrangement have become items that need to be

evaluated and controlled. Therefore, the integration of material science, condensed matter physics, chemistry, analytical technology, and equipment/process technology [9–13] will become an indispensable part of surface technology progress more than ever.

The paper proposed the fabrication process and thermal behavior of several types of powder coatings, based on magnesia, boron oxide, silicon oxide, and zinc, prepared by thermal spray methods—plasma and flame thermal spraying—which can find applications in the automotive industry. The ceramic film fabricated by spray technology has a network microstructure between the thermal insulation layer and the base material, and covers the thermal insulation layer and the base material with spray technology to improve the efficiency of the gas turbine and suppress heat dissipation of high-temperature components to save energy. The technology can alleviate the difference in thermal expansion, and the insulation layer contains many spherical or layered pores, which reduce the thermal conductivity.

As mentioned above, in various industrial fields, surface technology and products applying it are diversifying and becoming more and more important. The study of surface technology is also the key to solving environmental problems that are being solved on a global scale, which is the mission we must fulfill.

2. Materials and Methods

2.1. Experiment Material

2.1.1. SUS304 Substrate

In this study, SUS304 is used as substrate with a size of 30 mm × 30 mm × 3 mm (obtained from Nippon Steel Corporation in Tokyo, Japan). SUS304 is a typical austenitic stainless steel with excellent corrosion resistance, toughness, ductility, workability, weldability, and a wide range of uses. It is a sort of chromium-nickel-based stainless steel with 18% Cr-8% Ni as the main component and austenite with excellent corrosion resistance as the metal structure. Table 1 shows the chemical compositions of SUS304. In our research, SUS304 substrates are cut into 10 mm samples and ground with less than 50 μm roughness. In order to remove the impurities on the surface, samples are cleaned by the mixture of acetone and ethanol (1:1) with ultrasonic cleaning machine for 3 min, and then washed and dried.

Table 1. SUS304's chemical compositions (JIS standard).

Compositions	C	Si	Mn	P	S	Ni	Cr	Fe
Weight (%)	≤0.08	≤1.00	≤2.00	Max0.045	Max0.045	8.00–10.50	18.00–20.00	Balance

2.1.2. Thermal Spray Material Design

In this study, the coating is made by the thermal spray method. MgO powder is used as the main ingredient of coating material. Besides that, B₂O₃, SiO₂, and Zn are mixed with MgO in different proportions. Then, the mixed powder is crushed and sintered at 400–450 °C and then crushed again. The powder sizes are listed as follows:

- The size of MgO powder is 74 μm;
- The size of B₂O₃ powder is 48 μm;
- The size of SiO₂ powder is 65 μm;
- The size of Zn powder is 48 μm.

Different proportions are discussed and compared in this paper, and the compositions of spraying materials are shown in Table 2. In this paper, compositions are all expressed by percentage of weight (wt.%). All types of materials are analyzed with 100, 200, 300, and 500 μm, which are respectively expressed by X.1, X.2, X.3, and X.4.

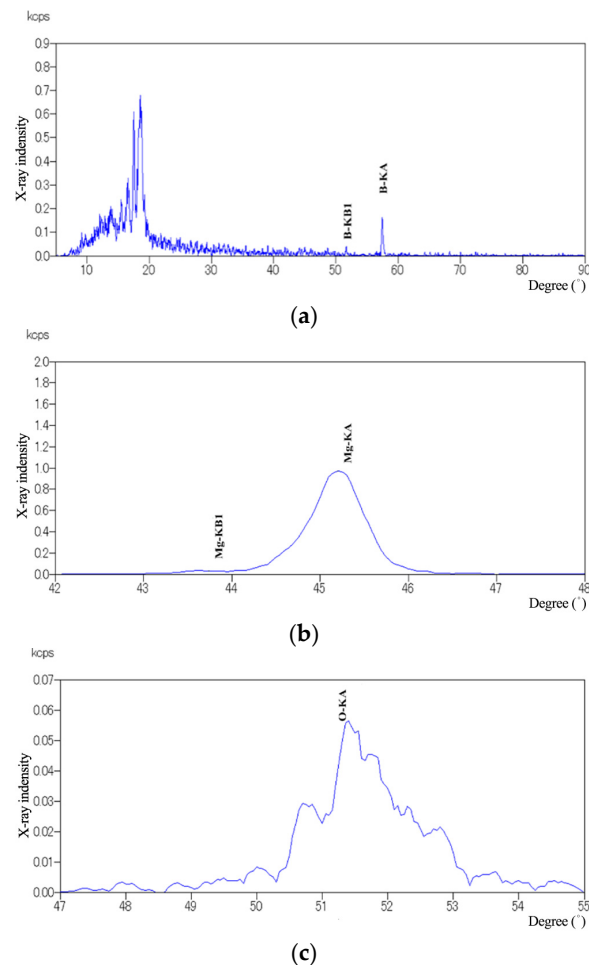
Table 2. Compositions of spray materials.

Compositions of Spray Material (wt.%)					Spraying Method	Film Thickness (μm)
No.	MgO	B ₂ O ₃	SiO ₂	Zn		
A	85	15	0	0	Plasma spraying	
B1	80	15	0	5		
B2	75	15	0	10		
B3	70	15	0	15	Flame spraying	100
C1	50	10	35	5		200
C2	50	10	30	10		300
C3	50	10	25	15		500

2.2. Fluorescence Spectroscopy Analysis of Spray Materials

In this section, X-ray fluorescence spectroscopy test is utilized to analyze the composition of thermal spray material prepared in Section 2.1, which is used to confirm the final percentage of each composition (carried on Regaku Corporation ZSX Primus II, Tokyo, Japan). In our research, $K\alpha$ and $K\beta$ X-ray are both used for analysis, and the identification KA and KB in all figures represent $K\alpha$ and $K\beta$ X-rays, respectively.

Here, the material A is taken as an example to demonstrate the result of X-ray analysis. Figure 1 is the power spectrum of the fluorescent X-ray qualitative analysis of composite powder A and shows the X-ray intensity of each element.

**Figure 1.** Cont.

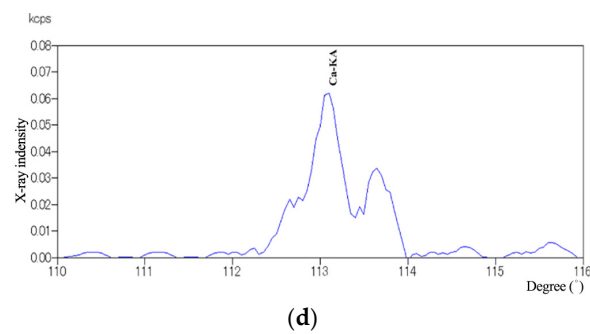


Figure 1. Fluorescence X-ray analysis diagram of A: (a) B-K α -K β ; (b) Mg-K α ; (c) O-K α ; (d) Ca-K α .

As shown in Figure 1, the peaks of elements such as Mg, B, O, and Ca are clearly displayed, and the amount of added elements is clarified based on the peak intensity of each element. Table 3 is the analysis results by X-rays for all types of materials.

Table 3. Composition analysis of powders by X-ray.

Component	Composition						
	A	B1	B2	B3	C1	C2	C3
	Weight (%)						
MgO	82.90	76.78	76.78	72.55	48.25	47.13	47.58
CaO	2.14	2.50	2.50	2.41	2.33	2.44	2.42
B ₂ O ₃	14.96	15.10	15.10	14.80	9.44	9.95	9.68
SiO ₂	0	0	0	0	34.83	30.19	25.51
Zn	0	5.63	5.63	10.25	5.15	10.27	14.81

2.3. Thermal Spray Method and Process

The purpose of this research is to provide a thermal insulation material, with its manufacturing method, that can be applied to plasma thermal spraying, flame thermal spraying, and form a film with a thermal insulation effect on the surface of the substrate, and to provide a thermal insulation film composed of thermal insulation and the insulation film's forming method.

In the previous section, the composition and proportion design of the spray powder in this paper are given. The powder can be coated on the substrate by plasma thermal spray (conducted by TAFA model by Praxair Surface Technologies, Indianapolis, IN, USA) and flame thermal spray (carried out on Castolin Eutectic CastoDyn DS8000, Lausanne, Switzerland), forming a layer of heat insulation film on the surface of the substrate, which can achieve excellent heat insulation effect. This section gives the specific operation process of the thermal spraying.

Before thermal spray, treat the surface of the substrate:

- Surface cleaning: the surface is cleaned with trichloroethylene solution before prior deposition.
- Surface pre-processing: the substrate is polished and cleaned on a grinder, and the corners are rounded.
- Surface roughness: The surface of the substrate must have a certain degree of roughness to improve the strength of the coating and the substrate.
- Surface preheating: flame is used to preheat the substrate, and the preheating temperature is 100–150 °C.

3. High Temperature Insulation Performance Evaluation

3.1. Experimental Device and Principle

In this study, a heating device is used to heat the center of SUS304 with coating under greenhouse conditions. The heating temperature is about 300 to 400 °C. The flame apex is

maintained 5 to 10 cm far from the center of the alloy. Heating continues for 75 min, and vertical photos are taken every 15 min by an infrared thermal instrument (TVS-700, NEC Corporation, Tokyo, Japan) to analyze the temperature changes of the points on the surface and the points on the coated surface based on the heat distribution map. Figure 2 is the schematic diagram of experiment equipment.

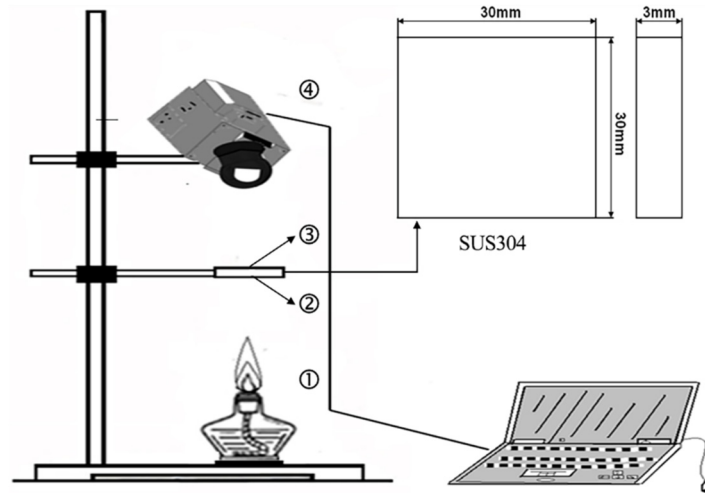


Figure 2. Self-made test device for high temperature insulation performance (heating temperature: 300–400 °C). (① Heating equipment; ② SUS304; ③ Coating surface; ④ Infrared thermal instrument (TVS-700)).

3.2. Experiment Results

3.2.1. Heat Distribution Measurement

This section takes the A.1 as an example to give the analysis results by the heat distribution diagram for 75 min. Similarly, thermal distribution analysis can be done for all types of materials. Figures 3–5 show the heat distribution maps of A.1 at different time.

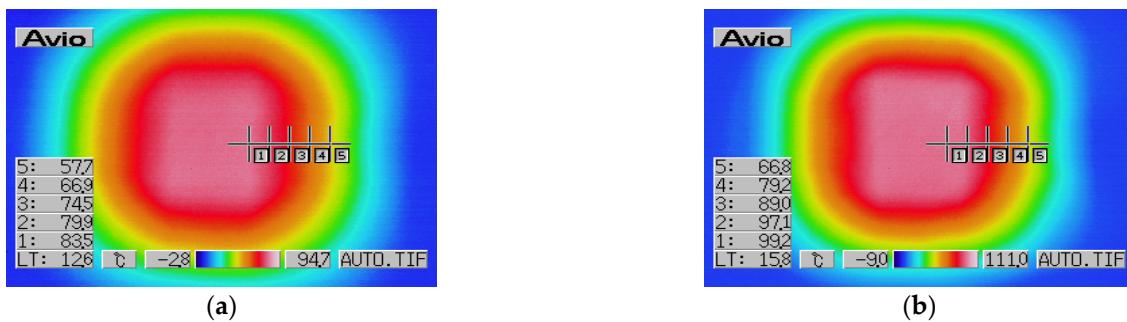


Figure 3. Heat distribution of the center point of 100 μm thickness at 15 min: (a) Coating plane; (b) SUS304 plane.

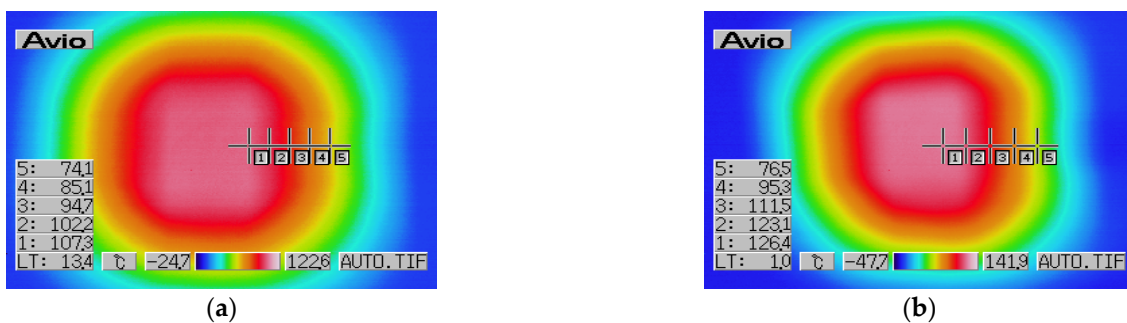


Figure 4. Heat distribution of the center point of 100 μm thickness at 30 min: (a) Coating plane; (b) SUS304 plane.

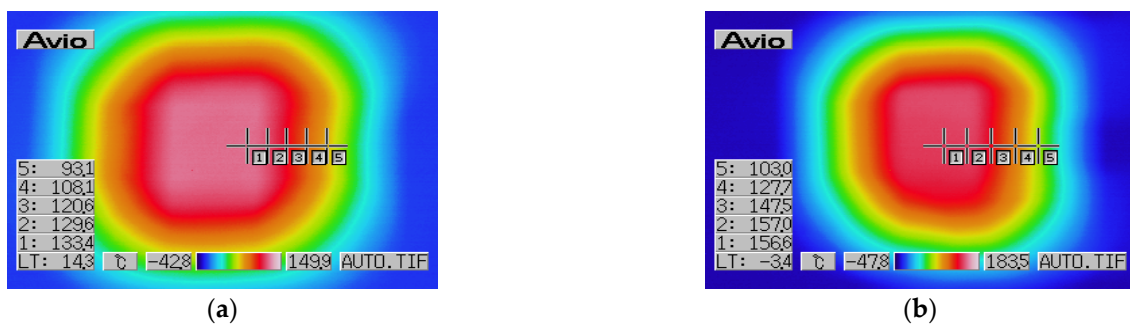


Figure 5. Heat distribution of the center point of 100 μm thickness at 45 min: (a) Coating plane; (b) SUS304 plane.

3.2.2. Analysis of Heat Distribution Results

According to the analysis of the heat distribution, the temperature changes in the high temperature environment can be compared for the different thermal spray layer thicknesses of each composition. Firstly, the high-temperature thermal insulation performance analysis of A is given in Figure 6.

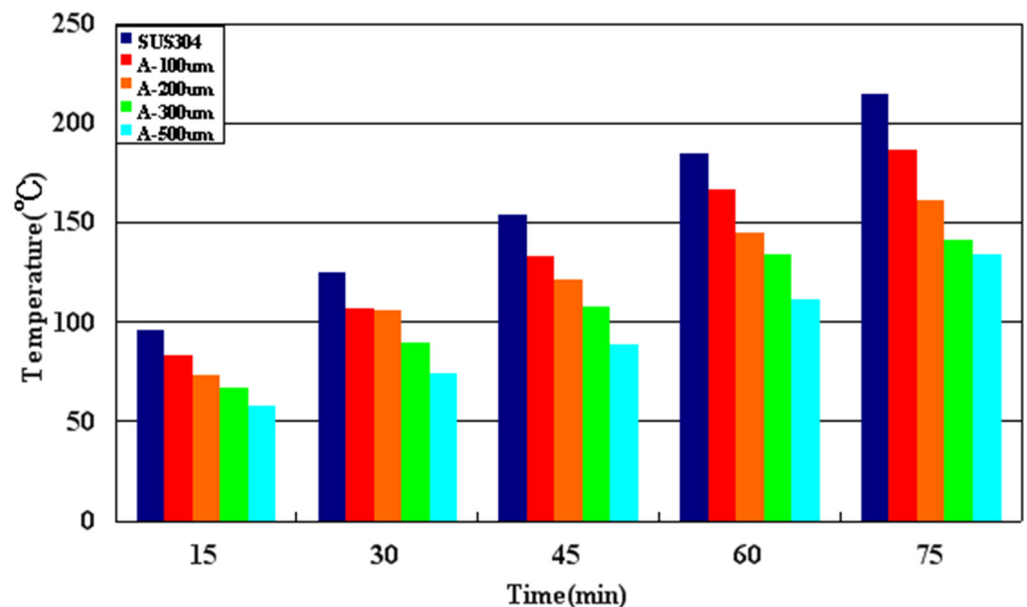


Figure 6. The temperature change analysis of A.

According to Figure 6 and Table 4, A.4 has the best high temperature insulation performance when the thickness is 500 μm . The temperature change is 58.1–134 $^{\circ}\text{C}$, and the temperature difference change is 35.7–75.8 $^{\circ}\text{C}$.

Table 4. The temperature difference between the surface of SUS304 and the coating surface of A.

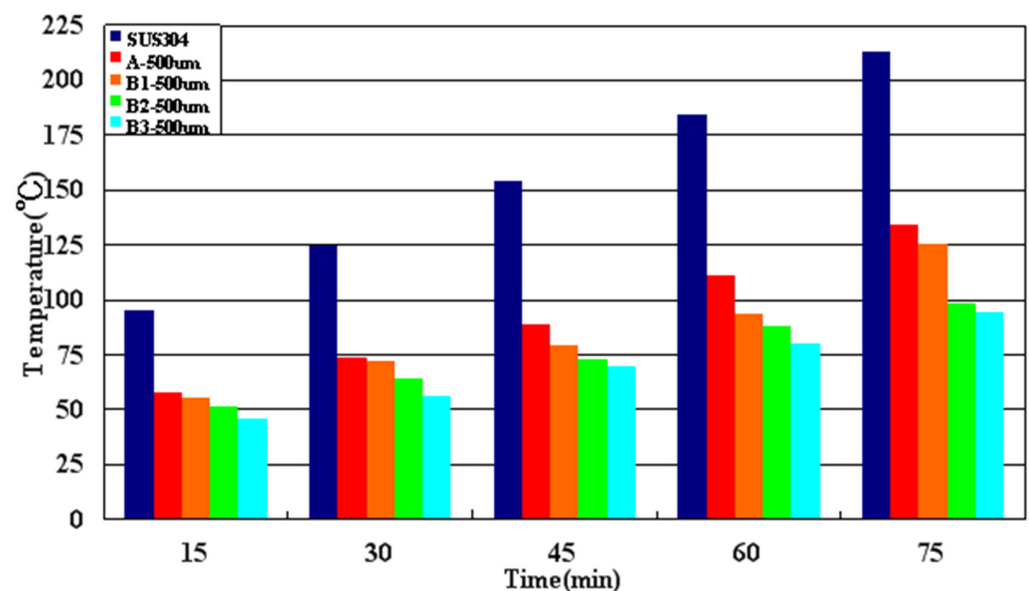
Time (min)	Temperature Difference ($^{\circ}\text{C}$)			
	A.1	A.2	A.3	A.4
15	15.7	22.5	28.8	35.7
30	19.1	19.5	36.0	46.2
45	23.2	33.4	44.9	60.8
60	24.6	42.6	50.3	63.8
75	32.3	51.8	68.8	75.8

Similarly, all type B material are also analyzed for 75 min to observe surface temperature. The data are summarized in Table 5.

Table 5. The temperature difference between the surface of SUS304 and the coating surface of B.

Coating Surface of B	Temperature Difference (°C)				
	15 min	30 min	45 min	60 min	75 min
B1.1	21.8	22.2	36.2	42.9	44.7
B1.2	26.5	19.9	42.1	56.6	55.0
B1.3	34.2	40.0	47.6	50.5	74.2
B1.4	36.9	47.2	68.3	93.4	83.2
B2.1	25.2	28.3	44.5	49.6	42.8
B2.2	27.7	33.3	54.4	64.7	64.7
B2.3	37.3	52.7	60.6	76.4	84.6
B2.4	41.3	58.3	81.4	93.4	103.4
B3.1	28.1	34.9	49.9	46.1	49.8
B3.2	35.0	38.2	57.1	71.4	69.4
B3.3	45.9	59.3	70.7	87.0	95.0
B3.4	48.6	69.9	86.1	107.4	123.6

Take the best thickness of the above four types of thermal spray powders as 500 μm , and compare their high-temperature thermal insulation performance as shown in Figure 7.

**Figure 7.** The temperature change analysis diagram of the center point of the SUS304 surface and the coating surface of 500 μm A and B.

4. Low Temperature Insulation Performance Evaluation

4.1. Experimental Device and Principle

In this study, a heating device is used to heat the performance of C under greenhouse conditions. The heating temperature is about 100 $^{\circ}\text{C}$, and the center of SUS304 is heated persistently. The measurement method and principles in low temperature experiments are similar to those in high temperature experiments. The flame apex is maintained 5 to 10 cm far from the center of the alloy. Heating continues for 75 min, and vertical photos are taken every 15 min by an infrared thermal instrument to analyze the temperature changes of the points on the surface and the points on the coated surface based on the heat distribution map. Figure 8 is the schematic diagram of experiment equipment.

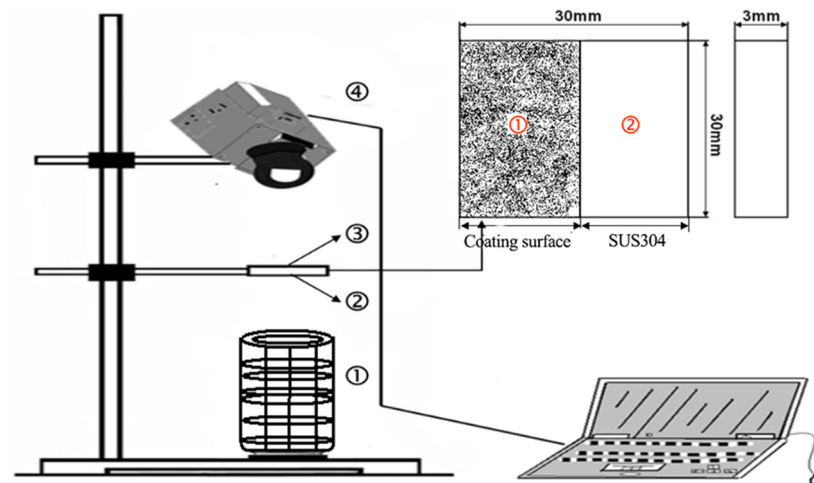


Figure 8. Self-made test device for low temperature insulation performance (heating temperature: 100 °C). (① Heating equipment; ② SUS304; ③ Coating surface; ④ Infrared thermal instrument (TVS-700)).

4.2. Experimental Results

4.2.1. Heat Distribution Measurement

The thermal insulation performance analysis of C1 with 100 μm thickness is given as an example in Figure 9.

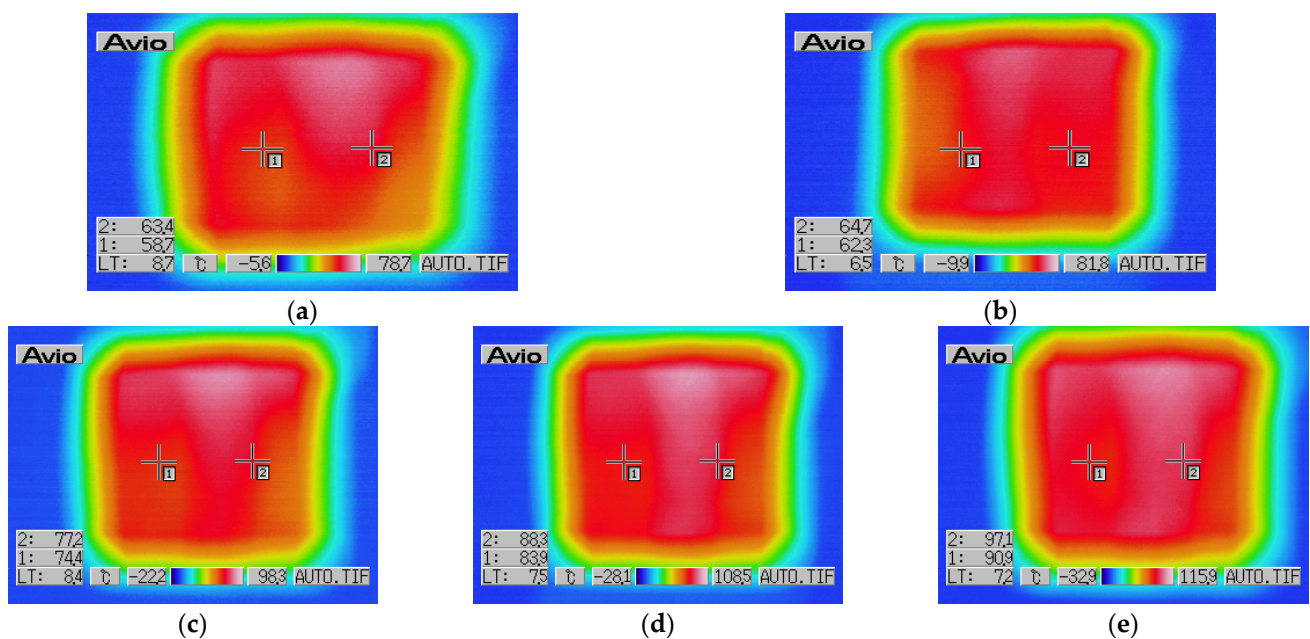


Figure 9. Heat distribution map of C1.1: (a) 15 min; (b) 30 min; (c) 45 min; (d) 60 min; (e) 75 min.

4.2.2. Analysis of Heat Distribution Results

According to the analysis of the heat distribution, the temperature changes in the high temperature environment can be compared for the different thermal spray layer thicknesses of each composition. Firstly, the high-temperature thermal insulation performance analysis of C1 is given in Figure 6.

According to Figure 10 and Table 6, C1.4 has the best low temperature insulation performance when the thickness is 500 μm . The temperature change is 42.6–68.6 °C. The temperature difference is 18.5–26.4 °C.

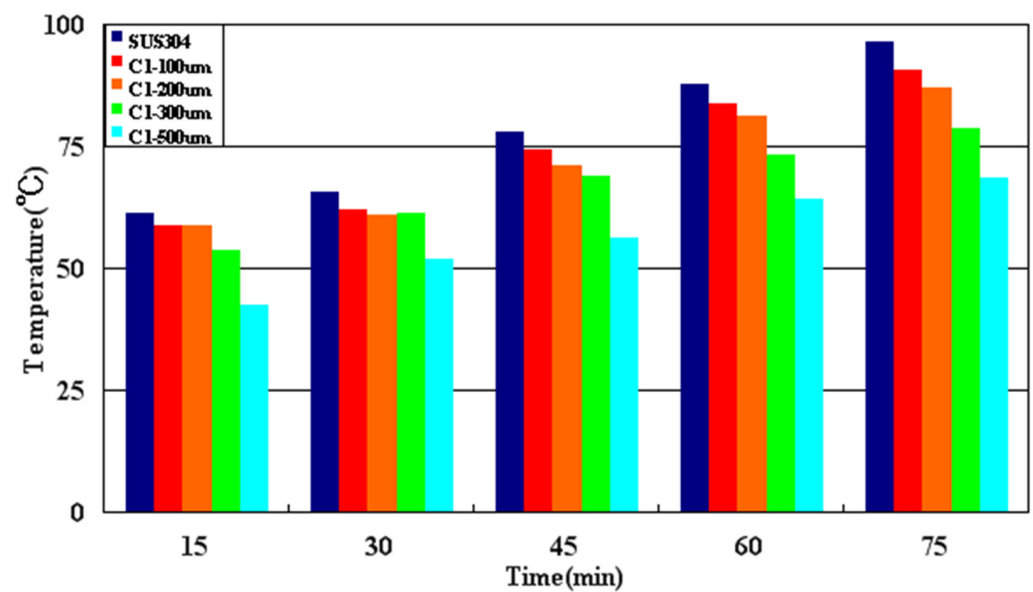


Figure 10. The temperature change analysis of C1.

Table 6. The temperature difference between the surface of SUS304 and coating surface of C.

Time (min)	Temperature Difference (°C)			
	C1.1	C1.2	C1.3	C1.4
15	4.7	3.9	6.5	18.5
30	2.4	4.4	4.3	14.7
45	2.8	6.7	9.9	22.1
60	4.4	6.0	15.4	23.1
75	6.2	10.0	17.9	26.4

Similarly, all types of C material are also analyzed for 75 min to observe surface temperature. The data are summarized in Table 7.

Table 7. The temperature difference between the surface of SUS304 and coating surface of C.

Coating Surface of C	Temperature Difference (°C)				
	15 min	30 min	45 min	60 min	75 min
C1.1	4.7	2.4	2.8	4.4	6.2
C1.2	3.9	4.4	6.7	6.0	10.0
C1.3	6.5	4.3	9.9	15.4	17.9
C1.4	18.5	14.7	22.1	23.1	26.4
C2.1	7.8	5.0	7.1	8.5	9.4
C2.2	6.7	5.8	7.7	14.2	14.7
C2.3	12.8	11.5	16.1	22.4	24.7
C2.4	20.3	19.9	28.5	30.7	37.3
C3.1	4.4	5.0	6.5	6.8	8.0
C3.2	5.1	5.2	9.2	10.8	13.0
C3.3	7.8	7.5	18.7	16.4	22.0
C3.4	20.3	19.4	22.5	22.1	27.1

Take the best thickness of the above three types of thermal spray powders as 500 µm, and compare their low-temperature thermal insulation performance as shown in Figure 11.

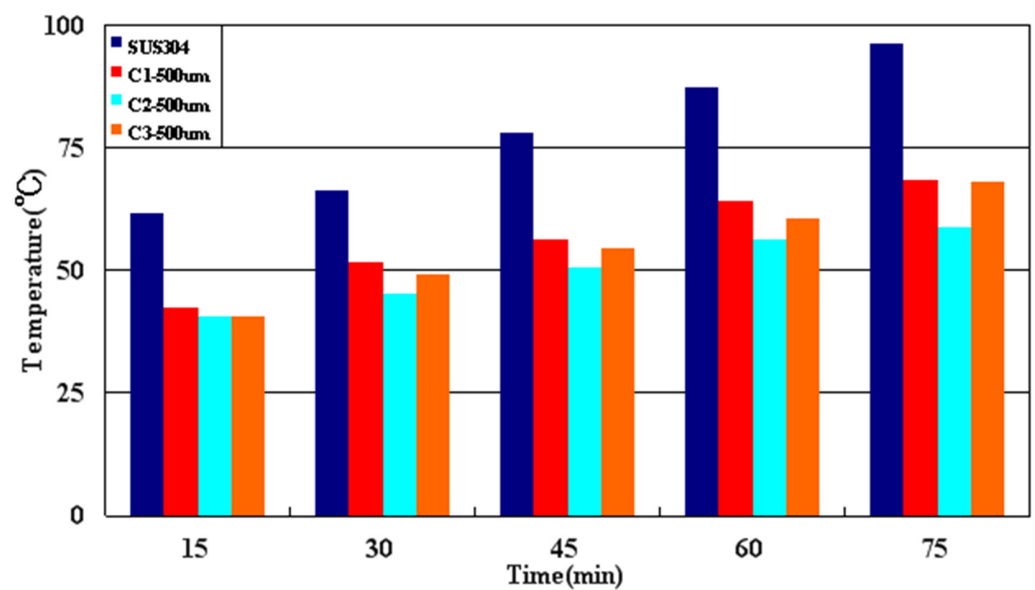


Figure 11. The temperature change analysis diagram of the center point of the SUS304 surface and coating surface of 500 μm C.

5. Conclusions

In this paper, based on substrate material SUS304, MgO-B₂O₃-Zn, and MgO-B₂O₃-SiO₂-Zn coatings are designed by plasma and flame thermal spray, which are used to suppress heat dissipation of high-temperature parts. It is found in the experiments that the best condition for the high temperature insulation performance comes from B3 at 500 μm , and the low temperature insulation performance comes from C2 at 500 μm .

By comparing the thermal images of coatings with different compositions, on the one hand, coating MgO-B₂O₃-Zn has significant performance under high temperature, and its performance grows along with the increase of Zn. On the other hand, in MgO-B₂O₃-SiO₂-Zn, SiO₂ also helps insulate heat conduction significantly, and the best percentage is 30%. However, the effect from SiO₂ is limited, and more and less SiO₂ both have a negative effect on heat insulation. Besides that, thermal insulation also grows along with the film thickness increases.

Author Contributions: Conceptualization, Z.Y.; Data curation, Y.S.; Formal analysis, P.M.; Methodology, D.J.; Software, Y.D.; Validation, W.F.; Writing—original draft, B.S.; Writing—review and editing, E.G. All authors have read and agreed to the published version of the manuscript.

Funding: This research received no external funding.

Institutional Review Board Statement: Not applicable.

Informed Consent Statement: Not applicable.

Data Availability Statement: Data sharing not applicable.

Conflicts of Interest: The authors declare no conflict of interest.

References

1. Barbezat, G. Advanced thermal spray technology and coating for lightweight engine blocks for the automotive industry. *Surf. Coat. Technol.* **2005**, *200*, 1990–1993. [[CrossRef](#)]
2. Xu, B.S. The remanufacturing engineering and automatic surface engineering technology. *Key Eng. Mater.* **2008**, *373–374*, 1–10. [[CrossRef](#)]
3. Kuroda, S.; Watanabe, M.; Kim, K.H.; Katanoda, H. Current status and future prospects of warm spray technology. *J. Therm. Spray Technol.* **2011**, *20*, 653–676. [[CrossRef](#)]
4. Burakowski, T.; Wierzchon, T. *Surface Engineering of Metals: Principles, Equipment, and Technologies*; CRC Press: Boca Raton, FL, USA, 1998.

5. Singh, H.; Sidhu, B.S.; Puri, D.; Prakash, S. Use of plasma spray technology for deposition of high temperature oxidation/corrosion resistant coatings—A review. *Mater. Corros.* **2007**, *58*, 92–102. [[CrossRef](#)]
6. Aneja, V.P.; Arya, S.P.; Kim, D.S.; Rumsey, I.C.; Arkinson, H.L.; Semunegus, H.; Bajwa, K.S.; Dickey, D.A.; Stefanski, L.A.; Todd, L.; et al. Characterizing ammonia emissions from swine farms in eastern north carolina: Part 1—Conventional lagoon and spray technology for waste treatment. *J. Air Waste Manag. Assoc.* **2008**, *58*, 1130–1144. [[CrossRef](#)] [[PubMed](#)]
7. Si, Y.; Wang, X.; Dou, L.; Yu, J.; Ding, B. Ultralight and fire-resistant ceramic nanofibrous aerogels with temperature-invariant superelasticity. *Sci. Adv.* **2018**, *4*, eaas8925. [[CrossRef](#)] [[PubMed](#)]
8. Dou, L.; Zhang, X.; Cheng, X.; Ma, Z.; Ding, B. Hierarchical cellular structured ceramic nanofibrous aerogels with temperature-invariant superelasticity for thermal insulation. *ACS Appl. Mater. Interfaces* **2019**, *11*, 29056–29064. [[CrossRef](#)] [[PubMed](#)]
9. Wang, H.; Xuan, Z.; Ning, W.; Li, Y.; Wu, H. Ultralight, scalable, and high-temperature-resilient ceramic nanofiber sponges. *Sci. Adv.* **2017**, *3*, e1603170. [[CrossRef](#)] [[PubMed](#)]
10. Dou, L.; Cheng, X.; Zhang, X.; Si, Y.; Yu, J.; Ding, B. Temperature-invariant superelastic, fatigue resistant, and binary-network structured silica nanofibrous aerogels for thermal superinsulation. *J. Mater. Chem. A* **2020**, *8*, 7775–7783. [[CrossRef](#)]
11. Huang, X.J.; Sun, J.H.; Jie, J.I.; Zhang, Y.; Wang, Q.S.; Zhang, Y. Flame spread over the surface of thermal insulation materials in different environments. *Chin. Sci. Bull.* **2011**, *56*, 1617–1622. [[CrossRef](#)]
12. Tao, G.; Jelle, B.P.; Sandberg, L.; Gustavsen, A. Monodisperse hollow silica nanospheres for nano insulation materials: Synthesis, characterization, and life cycle assessment. *ACS Appl. Mater. Interfaces* **2013**, *5*, 761–767. [[CrossRef](#)]
13. Lin, Y.; He, J. Recent progress in antireflection and self-cleaning technology—from surface engineering to functional surfaces. *Prog. Mater. Sci.* **2014**, *61*, 94–143.